ChemComm

Photoactivatable fluorophores for durable labelling of individual cells

Journal:	*ChemComm*
Manuscript ID	CC-COM-03-2021-001488.R1
Article Type:	Communication

ChemComm

COMMUNICATION

Photoactivatable fluorophores for durable labelling of individual cells

Received 00th January 20xx,
Accepted 00th January 20xx

DOI: 10.1039/x0xx00000x

www.rsc.org/

Hiroki Kashima[a], Mako Kamiya*[a], Fumiaki Obata[b], Ryosuke Kojima[a,c], Shotaro Nakano[b], Masayuki Miura[b] and Yasuteru Urano*[a,b,d]

We have designed and developed non-fluorescent, cell-permeable photoactivatable fluorophores, photoactivatable SPiDERs (paSPiDERs), which exhibit fluorescence activation upon light irradiation, accompanied with the generation a quinone methide intermediate that binds covalently to intracellular proteins. The fluorescence signal is durable for 24 hours, resistant to fixation and compatible with immunostaining, and selective cell labeling can be achieved at single-cell resolution.

Small-molecular photoactivatable fluorophores (PAFs, caged fluorophores) are fluorophores whose fluorescence is initially suppressed, but which can be photochemically converted to fluorescent molecules upon light irradiation[1, 2]. Various kinds of PAFs have been developed and they have proved to be powerful imaging tools for super-resolution imaging[3-5], and for tracking molecular and cellular dynamics with high spatiotemporal resolution.[4-8] For example, PAFs conjugated to dextran polymers had been used for selective cell labelling for long-term cell tracking or for cell-cell junctional coupling in vivo without genetic manipulations.[9-11] However, these conjugates need to be injected into cells. In contrast, small-molecular PAFs with thiol-reactive groups such as iodoacetamide (IAA)[2] are cell-membrane permeable, but can be retained in cells due to the formation of adducts with intracellular nucleophiles such as proteins. However, the promiscuous labelling of both target and non-target cells can potentially cause cytotoxicity in the absence of light irradiation (i.e., dark toxicity) due to the consumption of essential thiol-containing molecules in the cells. PAFs with intracellular esterase-reactive groups such as acetoxymethyl (AM) can also be retained in cells upon hydrolysis of the reactive group, but leakage of the fluorescent hydrolysis product from the cells during prolonged observation and/or fixation can be a problem. Although some recently reported fluorogenic photoaffinity labelling (PAL) probes enable fluorogenic labelling of specific protein without dark toxicity[12, 13], these PAL probes require relatively short-wavelength excitation for fluorescence imaging. Therefore, to achieve specific cell labelling and imaging with longer wavelength, there is still a need for cell-permeable PAFs that do not influence cell functions in the dark, but exhibit both fluorescence activation and acquisition of anchoring ability to intracellular proteins in response to light irradiation.

In this report, we describe new small-molecular PAFs that meet these requirements. To develop suitable molecules, we focused on our previously reported fluorescent probes for β-galactosidase (SPiDER-βGals)[14] and γ-glutamyltranspeptidase (4-CH_2F-HMDiEtR-gGlu)[15], which were designed so that reaction with the enzymes would produce electrophilic (aza)quinone methide intermediates that could be trapped by intracellular nucleophiles (Fig. S1). Based on this molecular design, we prepared rhodol-based photoactivatable SPiDER-1 (paSPiDER-1) and rhodamine-based paSPiDER-2 by replacing the β-galactosyl moiety of SPiDER-βGal and the γ-glutamyl moiety of 4-CH_2F-HMDiEtR-gGlu with a photolytic protecting group, the 4,5-dimethoxy nitrobenzyl group (DMNB) (Fig. 1a, Scheme S3). We selected DMNB as a caging group because of its relatively long absorbance[16, 17], so that uncaging could be achieved with a commonly used 405 nm laser. The resulting PAFs were expected to be initially non-fluorescent and cell-permeable, but to exhibit durable fluorescence activation in light-irradiated target cells via covalent binding to intracellular proteins.

To validate our design strategy, we first evaluated the optical properties of paSPiDERs in aqueous solution. As expected, the absorbance and fluorescence spectra at various pHs showed that paSPiDERs exhibited a pH-dependent equilibrium of intramolecular spirocyclization; they exist in the colored xanthene form with absorption and emission in the visible wavelength range at acidic pH, whereas they exist in the

[a] Graduate School of Medicine, The University of Tokyo, 7-3-1 Hongo, Bunkyo-ku, Tokyo 113-0033, Japan. E-mail: mkamiya@m.u-tokyo.ac.jp
[b] Graduate School of Pharmaceutical Sciences, The University of Tokyo, 7-3-1 Hongo, Bunkyo-ku, Tokyo 113-0033, Japan. E-mail: uranokun@m.u-tokyo.ac.jp
[c] PRESTO, Japan Science and Technology Agency, 4-1-8 Honcho, Kawaguchi, Saitama 332-0012, Japan.
[d] AMED CREST

† Electronic Supplementary Information (ESI) available: Synthetic procedures and characterization of new compounds, optical properties and imaging details.

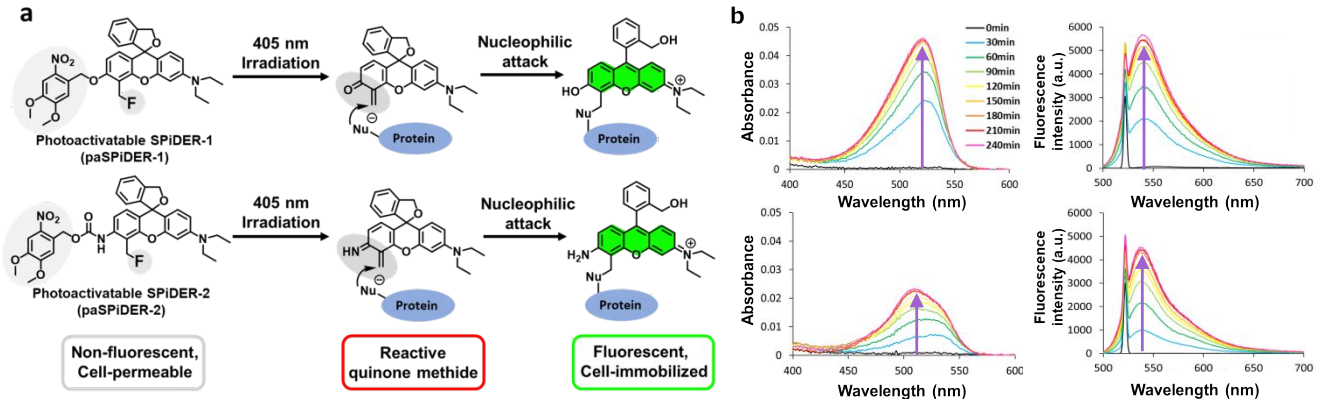

Fig. 1 (a) Molecular design of **paSPiDER-1** (upper) and **paSPiDER-2** (bottom), and the activation mechanism of fluorescence and binding ability to intracellular nucleophiles, such as proteins, by photo-irradiation so that the fluorescent products are immobilized in living cells. (b) Change of absorbance (left) and fluorescence (right) spectra of 1 μM solution of paSPiDER-1 (upper) and paSPiDER-2 (bottom) in 200 mM sodium phosphate buffer, pH 7.4, upon 405 nm light irradiation (18.3 or 19.3 mW/cm^2) for 4 hours.

Table 1. Photophysical properties of paSPiDERs and the putative photo-reaction products [a)]

	Abs$_{max}$ (nm)	Em$_{max}$ (nm)	ε (M^{-1}cm^{-1})	Φ_{fl}	pK_{cycl}	Brightness ($\varepsilon\times\Phi_{fl}$)
paSPiDER-1	493, 527[b)]	561, 601[b)]	52,000[b)]	0.01[b)]	3.4	520
paSPiDER-2	498, 533[b)]	570, 620[b)]	38,000[b)]	0.01[b)]	3.5	380
4-CH$_2$OH-HMDER	526[c)]	553[c)]	120,000[b)]	0.11[c)]	11.4[c)]	13,200
4-CH$_2$OH-HMDiEtR	534[d)]	558[d)]	100,000[b)]	0.04[d)]	9.6[d)]	4,000

[a]Absorption maximum (λ_{abs}), fluorescence emission maximum (λ_{em}), molar extinction coefficient (ε), fluorescence quantum yield (Φ_{fl}), equilibrium constant for intramolecular spirocyclization (pK_{cycl}), relative brightness ($\varepsilon\times\Phi_{fl}$). [b]Measured in 200 mM sodium phosphate buffer (pH 2.0). [c]Reference 14. [d]Reference 15.

colorless spirocyclic form at neutral and alkaline pHs. The values of pK_{cycl} (the pH at which the extent of spirocyclization is sufficient to reduce the absorbance of the compound to one-half of the maximum absorbance)[18] of paSPiDER-1 and paSPiDER-2 were calculated to be 3.4 and 3.5, respectively, indicating that these paSPiDERs mainly exist in the colorless and non-fluorescent form at the physiological pH of 7.4 (Fig. S2, Table 1). The fluorescence quantum yields (Φ_{fl}) of the open forms of paSPiDER-1 and paSPiDER-2 were also suppressed to 0.01, suggesting that the background fluorescence signal would be low. In contrast, the pK_{cycl} values of 4-CH$_2$OH-HMDER and 4-CH$_2$OH-HMDiEtR, the model reaction products of paSPiDER-1 and paSPiDER-2, were reported to be 11.4 and 9.6, respectively, indicating that they would mainly exist as the colored, fluorescent open forms at pH 7.4 (Φ_{fl} = 0.11 for 4-CH$_2$OH-HMDER and 0.04 for 4-CH$_2$OH-HMDiEtR). Taken together, these results indicate that the paSPiDERs function as highly fluorogenic PAFs.

We next examined the photoactivation properties of the paSPiDERs. When solutions of the paSPiDERs in 200 mM sodium phosphate buffer at pH 7.4 were illuminated with 405 nm light from a xenon source, we observed significant increases of absorption and fluorescence intensity in the visible region in a time-dependent manner, suggesting that the paSPiDERs were converted to the colored and fluorescent hydrolysis products (Fig. 1b). However, especially in the case of paSPiDER-2, we noticed that the absorption maximum shifted to shorter wavelength, depending on the irradiation time. In order to clarify the reason for this, we analysed the photoreaction solution by LCMS and found that 4-CH$_2$OH-HMDER and 4-CH$_2$OH-HMDiEtR (water adducts of the respective (aza)quinone methide intermediates) were mainly produced, but *N*-dealkylated products were also formed by light irradiation, presumably via oxidative *N*-dealkylation[19] (Fig. S4). The photoreaction solution of paSPiDER-2 contained a higher percentage of *N*-dealkylated by-products, which would explain the marked blue-shift in the absorption spectrum of paSPiDER-2 upon light irradiation, but we assumed that production of these *N*-dealkylated by-products would not be a problem for cell labelling. SDS-PAGE analysis of the photoreaction solution in the presence of bovine serum albumin (BSA) confirmed that photoactivated paSPiDERs can bind to BSA to produce fluorescent adducts (Fig. S5).

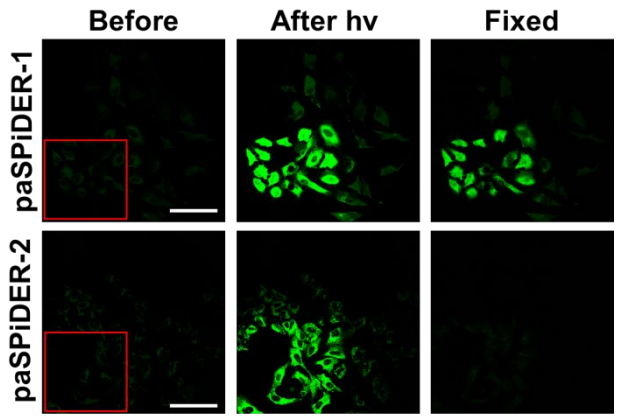

Fig. 2 Fluorescence images of A549 cells treated with 10 μM **paSPiDER-1** (**upper**) and **paSPiDER-2** (**bottom**) for 1 h, followed by 405 nm light irradiation and MeOH fixation. (left) before light irradiation, (middle) after light irradiation, (right) after MeOH fixation for 15 min. Red square: 405 nm light-irradiated region. The cell passage number is more than ten. Ex/Em = 525 nm/535–595 nm. Scale bars, 100 μm.

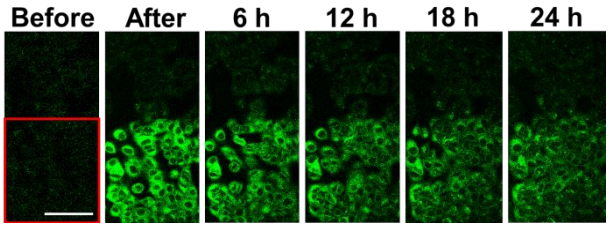

Fig. 3 Time-lapse fluorescence imaging of A549 cells treated with 10 μM **paSPiDER-1** for 1 h, followed by 405 nm light irradiation, for up to 24 h. Red square: 405 nm light-irradiated region. Ex/Em = 525 nm/535–595 nm. Scale bar, 100 μm.

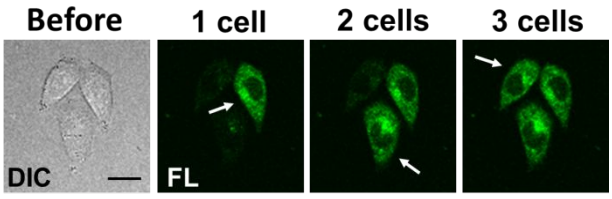

Fig. 4 Fluorescence and DIC images of A549 cells treated with 10 μM **paSPiDER-1** for 1 h, followed by photoactivation of each cell by 405 nm light. Arrows indicate 405 nm light-irradiated cell at each time point. Ex/Em = 525 nm/535–595 nm. Scale bar, 20 μm.

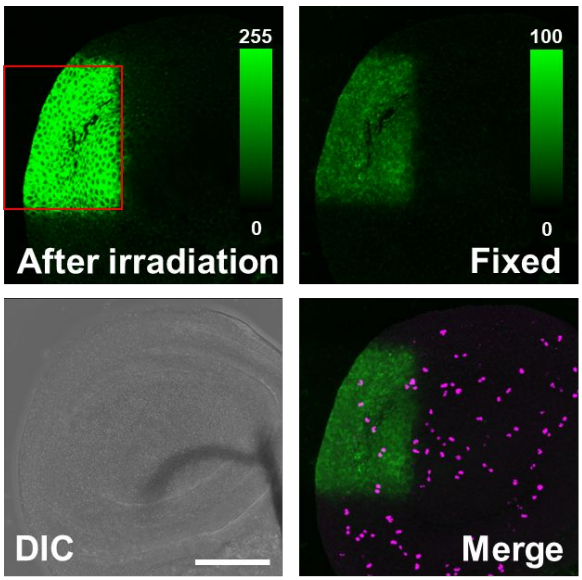

Fig. 5 Ex vivo cell labeling of *Drosophila* tissue. *Drosophila* wing disc was treated with 50 μM paSPiDER-1, followed by 405 nm light irradiation. Activation of the green fluorescent signal derived from paSPiDER-1 was observed only in the light-irradiated area (red square). Then, the tissue was fixed with 4% PFA and subjected to immunostaining with anti-phospho-histone H3 antibody (magenda). Ex/Em = 488 nm/500–550 nm. Scale bar, 75 μm.

Next, in order to determine whether paSPiDER-1 and paSPiDER-2 have cell membrane permeability and can function as PAFs in live cells, we applied them to cultured A549 cells (human lung adenocarcinoma-derived cell lines), followed by 405 nm laser light irradiation. We observed a significant fluorescence increase in cells in the light-irradiated region in both cases, demonstrating that the paSPiDERs are cell membrane permeable and do function as PAFs in live cells (Fig. 2). Further, the obtained fluorescence signals were resistant to 4% PFA fixation, which is known to induce cross-linking of intracellular components, as in the case of our previously reported SPiDER-βGal and 4-CH_2F-HMDiEtR-gGlu (Fig. S6). In contrast, fixation treatment with methanol, which is known to induce protein precipitation, reduced the fluorescence signal from paSPiDER-2, though the fluorescence signal from paSPiDER-1 was well maintained (Fig. 2). The results appeared to be independent of the passage number of the cells (Fig. S7). As it was reported that MeOH fixation leads to a more severe loss of cell components than PFA fixation[20], this result suggests that activated paSPiDER-1 preferentially labels protein fractions resistant to MeOH fixation, as compared with paSPiDER-2, due to the difference in the generation rate or reactivity of quinone methide and azaquinone methide intermediates. We did not characterize what nucleophiles bind to the quinone methide intermediates, but it has been reported that quinone methide intermediates are trapped by cysteine thiol, lysine ε-amine, and histidine imidazole[21-23]. Therefore, the intermediates produced from paSPiDERs would likely have been trapped by free nucleophilic amino acids, glutathione, and water, in addition to the protein fraction. Based on the above results, we focused on paSPiDER-1 for further experiments.

In order to evaluate the practical utility of paSPiDER-1, we next examined whether the activated fluorescence signal of paSPiDER-1 can be tracked for 24 hours (Fig. 3, S8). Although the fluorescence intensity gradually decreased, the cell region fluorescently labelled with paSPiDER-1 could be easily recognized even after 24 h, which suggests that paSPiDER-1 would be suitable for long-term cell tracking. Further, we evaluated whether selective cell labelling can be achieved by pinpoint light irradiation of single cells. Indeed, fluorescence activation was observed only in individually light-irradiated cells, enabling us to perform sequential cell labelling at single-cell resolution (Fig. 4, S9). We also confirmed that the fluorescence signals activated locally in cells diffused throughout the cytoplasm, suggesting that fluorescence labelling of subcellular regions with paSPiDER-1 would not be feasible (Fig. S10).

We further examined the toxicity of paSPiDER-1. First, we measured the dark toxicity of paSPiDER-1 compared to that of CellTracker™ Red CMTPX dye, which is a commercially available cell-tracking dye with a thiol-reactive chloromethyl group, thus we used as a model comparison dye (Figure S11). We confirmed that paSPiDER-1 did not show obvious cytotoxicity at the concentrations we used for cellular imaging, whereas CellTracker™ Red showed cytotoxicity in a concentration-dependent manner, owing to promiscuous labelling of intracellular nucleophiles such as proteins. These results demonstrated that the molecular design of paSPiDER-1 is effective to suppress dark toxicity compared to PAFs with thiol-reactive groups. Second, we evaluated the phototoxicity of paSPiDER-1 by staining paSPiDER-1-treated and light-irradiated cells with the cell-impermeant viability indicator, ethidium homodimer-1 (EthD-1), which stains only dead cells in red. We observed no marked staining with EthD-1 in paSPiDER-1-treated and light-irradiated cells for at least the following 15 h, whereas strong red staining was observed in fixed cells (Fig. S12-S13). These results indicate that the phototoxicity of paSPiDER-1 is

low, and suggest that paSPiDER-1 would not substantially affect the physiological functions of live cells. Therefore, paSPiDER-1 should be suitable for live-cell fluorescence labelling experiments.

Finally, to confirm the applicability of paSPiDER-1 in live tissues, we performed ex vivo fluorescence labelling of *Drosophila melanogaster* tissues. We applied paSPiDER-1 to live larval wing disc, a precursor structure of a part of the adult thorax including the wing. After incubation for 30 min, 405 nm laser light irradiation significantly increased the fluorescence intensity only in the irradiated area, indicating that paSPiDER-1 works as a PAF in live tissues (Fig. 5). Further, the tissue was fixed with 4% PFA and subjected to immunostaining with anti-phospho-histone H3 antibody. Although the fluorescence signal intensity derived from paSPiDER-1 was decreased following fixation, the fluorescently labelled cell region could still be clearly recognized, demonstrating the high compatibility of paSPiDER-1 with immunostaining.

In conclusion, we have developed cell-permeable PAFs, paSPiDERs, which were designed to show simultaneous activation of fluorescence and covalent binding ability to intracellular nucleophiles in response to light irradiation. Light activation of paSPiDER-1 produced fluorescence signals that were both resistant to MeOH fixation and durable, enabling long-term observation. Selective cell labelling can be achieved at single-cell resolution, and paSPiDER-1 labelling is compatible with immunostaining. For in vivo applications, two-photon uncaging would be useful to achieve deeper tissue penetration, but two-photon activation of paSPiDERs in their present forms would be difficult due to the low sensitivity of DMNB caging groups to two-photon excitation[17, 24]. However, we expect it would be possible to prepare paSPiDER analogues suitable for two-photon activation by replacing the DMNB moiety with other caging groups having a high two-photon cross-section. Such analogues should be suitable for long-term cell tracking in vivo, such as cell lineage analysis, and in combination with immunostaining, should be versatile tools for studying cellular dynamics or cell fate.

This research was supported in part by AMED under grant number JP19gm0710008 (to Y.U.) and JP21gm5010001 (to M.M.), by JST/PRESTO grant JPMJPR14F8 (to M.K.), by MEXT/JSPS KAKENHI grants JP16H02606, JP26111012, and JP19H05632 (to Y.U.) and JP15H05951 “Resonance Bio”, JP19H02826, JP19K22242, and 20H05724 (to M.K.), and 20H05726 (to F.O.) and 16H06385 (to M.M.), by JSPS Core-to-Core Program (grant number JPJSCCA20170007), A. Advanced Research Networks, by Japan Foundation for Applied Enzymology (to M.K.), and The Naito Foundation (to M.K.), as well as a stipend from the World-leading Innovative Graduate Study Program for Life Science and Technology (WINGS-LST) (to H.K. and S.N.).

Conflicts of interest

There are no conflicts to declare.

Notes and references

1. T. J. Mitchison, K. E. Sawin, J. A. Theriot, K. Gee and A. Mallavarapu, in *Methods in Enzymology*, Academic Press, 1998, vol. 291, pp. 63-78.
2. D. Puliti, D. Warther, C. Orange, A. Specht and M. Goeldner, *Bioorg Med Chem*, 2011, **19**, 1023-1029.
3. J. B. Grimm, T. Klein, B. G. Kopek, G. Shtengel, H. F. Hess, M. Sauer and L. D. Lavis, *Angew Chem Int Ed Engl*, 2016, **55**, 1723-1727.
4. J. B. Grimm, B. P. English, H. Choi, A. K. Muthusamy, B. P. Mehl, P. Dong, T. A. Brown, J. Lippincott-Schwartz, Z. Liu, T. Lionnet and L. D. Lavis, *Nat Methods*, 2016, **13**, 985-988.
5. M. S. Frei, P. Hoess, M. Lampe, B. Nijmeijer, M. Kueblbeck, J. Ellenberg, H. Wadepohl, J. Ries, S. Pitsch, L. Reymond and K. Johnsson, *Nature Communications*, 2019, **10**, 4580.
6. Y. Zhao, Q. Zheng, K. Dakin, K. Xu, M. L. Martinez and W. H. Li, *J Am Chem Soc*, 2004, **126**, 4653-4663.
7. D. Maurel, S. Banala, T. Laroche and K. Johnsson, *ACS Chemical Biology*, 2010, **5**, 507-516.
8. S. Hauke, A. von Appen, T. Quidwai, J. Ries and R. Wombacher, *Chemical science*, 2017, **8**, 559-566.
9. D. J. Kozlowski, T. Murakami, R. K. Ho and E. S. Weinberg, *Biochemistry and Cell Biology*, 1997, **75**, 551-562.
10. K. R. G. S. W. J.Kozlowskib, *Bioorganic & Medicinal Chemistry Letters*, 2001, **11**, 2181-2183.
11. Y. M. Guo, S. Chen, P. Shetty, G. Zheng, R. Lin and W. H. Li, *Nat Methods*, 2008, **5**, 835-841.
12. S.-Y. Dai and D. Yang, *Journal of the American Chemical Society*, 2020, **142**, 17156-17166.
13. M. Cauwel, C. Guillou, K. Renault, D. Schapman, M. Bénard, L. Galas, P. Cosette, P.-Y. Renard and C. Sabot, *Chemical Communications*, 2021, **57**, 3893-3896.
14. T. Doura, M. Kamiya, F. Obata, Y. Yamaguchi, T. Y. Hiyama, T. Matsuda, A. Fukamizu, M. Noda, M. Miura and Y. Urano, *Angew Chem Int Ed Engl*, 2016, **55**, 9620-9624.
15. R. Obara, M. Kamiya, Y. Tanaka, A. Abe, R. Kojima, T. Kawaguchi, M. Sugawara, A. Takahashi, T. Noda and Y. Urano, *Angew Chem Int Ed Engl*, 2021, **60**, 2125-2129.
16. B. F. Jack H. Kaplan, III, and Joseph F. Hoffman, *Biochemistry*, 1978, **17**, 1929-1935.
17. T. M. D. a. H. C. Wilson, *Neuromethods*, 2011, **55**, 57-92.
18. M. Kamiya, D. Asanuma, E. Kuranaga, A. Takeishi, M. Sakabe, M. Miura, T. Nagano and Y. Urano, *J Am Chem Soc*, 2011, **133**, 12960-12963.
19. A. N. Butkevich, M. L. Bossi, G. Lukinavicius and S. W. Hell, *J Am Chem Soc*, 2019, **141**, 981-989.
20. A. J. Hobro and N. I. Smith, *Vibrational Spectroscopy*, 2017, **91**, 31-45.
21. S. B. T. b. Judy L. Bolton a, John A. Thompson, *Chemico-Biological Interactions*, 1997, **107**, 185-200.
22. D. H. Kwan, H. M. Chen, K. Ratananikom, S. M. Hancock, Y. Watanabe, P. T. Kongsaeree, A. L. Samuels and S. G. Withers, *Angew Chem Int Ed Engl*, 2011, **50**, 300-303.
23. J. Liu, S. Li, N. A. Aslam, F. Zheng, B. Yang, R. Cheng, N. Wang, S. Rozovsky, P. G. Wang, Q. Wang and L. Wang, *J Am Chem Soc*, 2019, **141**, 9458-9462.
24. G. Bort, T. Gallavardin, D. Ogden and P. I. Dalko, *Angew Chem Int Ed Engl*, 2013, **52**, 4526-4537.

